Insect Molecular Biology (2020) doi: 10.1111/imb.12657

Intracellular dynamics of polydnavirus innexin homologues

D. K. Hasegawa*‡, P. Zhang*† and M. W. Turnbull*†

*Department of Biological Sciences, Clemson University, Clemson, SC, USA; †Department of Plant and Environmental Sciences, Clemson University, Clemson, SC, USA; and ‡USDA-ARS, Crop Improvement and Protection Research Unit, Salinas, CA, USA

Abstract

Polydnaviruses associated with ichneumonid parasitoid wasps (Ichnoviruses) encode large numbers of genes, often in multigene families. The Ichnovirus Vinnexin gene family, which is expressed in parasitized lepidopteran larvae, encodes homologues of Innexins, the structural components of insect gap junctions. Here, we have examined intracellular behaviours of the *Campoletis sonorensis* Ichnovirus (CsIV) Vinnexins, alone and in combination with a host Innexin orthologue, Innexin2 (Inx2). QRT-PCR verified that transcription of CsIV *vinnexins* occurs contemporaneously with *inx2*, implying co-occurrence of Vinnexin and Inx2 proteins. Confocal microscopy demonstrated that epitope-tagged VinnexinG (VnxG) and VinnexinQ2 (VnxQ2) exhibit similar subcellular localization as *Spodoptera frugiperda* Inx2 (*Sf*-Inx2). Surface biotinylation assays verified that all three proteins localize to the cell surface, and cytochalasin B and nocodazole that they rely on actin and microtubule cytoskeletal networks for localization. Immunomicroscopy following co-transfection of constructs indicates extensive co-localization of Vinnexins with each other and *Sf*-Inx2, and live-cell imaging of mCherry-labelled Inx2 supports that Vinnexins may affect *Sf*-Inx2 distribution in a Vinnexin-specific fashion. Our findings support that the Vinnexins may disrupt host cell physiology in a protein-specific manner through altering gap junctional intercellular channel communication, as well as indirectly by affecting multicellular junction characteristics.

Keywords: *Campoletis sonorensis* Ichnovirus, gap junction, innexin, polydnavirus, vinnexin, cytoskeleton.

Introduction

Understanding the mechanisms that enable multicellular coordination is essential to comprehending the structures and functions of insect biology. Similarly, understanding the mechanisms that disrupt multicellular and individual cell behaviours can provide insight to some of the steps that drive pathological processes. While much focus in insect science has been on secreted receptor-ligand signalling pathways, direct transfer of molecules by gap junctions is a requisite for much of life's complexity in nearly all animals, including insects. Physiological functions continue to be ascribed to gap junctions in insects, although much regarding their regulation and physiology remains unknown. Greater focus on the behaviour of gap junctions and their foundational units is thus needed, including an understanding of gap junction behaviour during pathological states.

Insect gap junctions are formed by polymers of Innexin proteins: six Innexin proteins form a hemichannel, which localizes to the cell surface, where interaction with an adjacent cell's hemichannel may lead to formation of a gap junction (Bauer et al., 2005; Hasegawa and Turnbull, 2014). Innexin-comprised hemichannels in insects permit transfer of small molecules directly between cytoplasm of adjacent cells via gap junctions, or the cytoplasm and extracellular environment in the case of unapposed hemichannels (Luo and Turnbull, 2011; Pang et al., 2015). Insect genomes sequenced to date appear to encode five to eight *innexin* loci (Hasegawa and Turnbull, 2014), with complex patterns of expression suggesting that there are protein- and hemichannel-specific functions (Stebbings et al., 2002; Hong et al., 2009). Protein sequence affects Innexin function and cellular behaviour, in part determining potential protein–protein

First published online 7 August 2020.

Correspondence: Matthew Turnbull, Department of Biological Sciences, Clemson University, Clemson, SC, USA. Tel.: +864 656 5038; fax: +864 656 4960; e-mail: turnbul@clemson.edu

interactions and thus the ability to form hemichannels and gap junctions with more than one Innexin type (Bauer et al., 2003; Bauer et al., 2004; Bohrmann and Zimmermann, 2008). This in turn likely affects pore characteristics including width and charge, affecting hemichannel selectivity and structure, open/close state and even cellular localization (Depriest et al., 2011; Holcroft et al., 2013).

The Polydnaviruses are a paraphyletic group of large dsDNA viruses associated with several subfamilies of braconid (the viruses are known as Bracoviruses) and ichneumonid (Ichnoviruses) parasitoid wasps (Bezier et al., 2009; Volkoff et al., 2010; Drezen et al., 2014; Beliveau et al., 2015). All members of an associated wasp species are infected by a species-specific Polydnavirus: the virus is integrated into the wasp germ line genome, and inherited vertically as a provirus. Proviral loci are replicated and encapsidated in the pupal ovary, then transferred during parasitization to the host hemocoel (typically of larval lepidopteran) whereupon the encapsidated virus infects virtually all tissues. Subsequent Polydnavirus gene expression induces numerous immune and metabolic alterations that generally are essential to parasitoid offspring development (Cui et al., 2000; Bitra et al., 2016). Many Polydnavirus genes are part of gene families, of which there are numerous examples in each Polydnavirus genome (Espagne et al., 2004; Webb et al., 2006; Lapointe et al., 2007; Tanaka et al., 2007; Strand and Burke, 2013; Doremus et al., 2014b). In the case of Ichnoviruses, the functional consequences of multigene families are largely unclear: members could be functionally redundant, or play complementary functional roles in different tissues and/or hosts.

All Ichnoviruses (IVs) sequenced to date encode homologues of Innexins, known as Vinnexins (Virus Innexins) (Hasegawa and Turnbull, 2014). There are four vinnexin genes (*vnxD*, *vnxG*, *vnxQ1*, *vnxQ2*) in the *Campoletis sonorensis* Ichnovirus (CsIV) genome, which previously have been shown to form functional gap junctions (Turnbull et al., 2005; Marziano et al., 2011). In paired *Xenopus laevis* oocytes, the CsIV vinnexins differentially affect the reliability and conductance characteristics of gap junctions when co-expressed with *Spodoptera frugiperda* Innexin2 (*Sf*-Inx2) (Marziano et al., 2011), suggesting that the proteins encode different competence to interact with *Sf*-Inx2 or affect channel characteristics, or modify *Sf*-Inx2 physiology through another means. In another heterologous system – transgenic *Drosophila melanogaster* – global *vnxG* expression was embryonic lethal, while expression of the other three CsIV Vinnexins had no effect on fly viability; ectopic larval gut expression likewise had no observable effect for any of the Vinnexins other than *vnxG*, which was pupal lethal (Hasegawa et al., 2017). In experiments to date in lepidopteran cells, the different Vinnexins exhibit protein-specific degrees of pathophysiology: VnxG and VnxQ2 are both associated with cell membrane depolarization and cytoplasmic alkalization with VnxG acting to a greater degree (Zhang and Turnbull, 2018), and VnxQ1 and VnxQ2 reduced cell area while increasing circularity relative to controls, while VnxG had no effect on morphology (Hasegawa et al., 2017).

It is currently unclear, although, whether Vinnexins act (only) through altered gap junction intercellular communication, or by interaction with other cellular proteins. Misexpression of insect Innexins can result in altered distribution of other intercellular junctions, such as adherens junctions, as well as signalling molecules such as β-catenin (Lehmann et al., 2006); these molecules in turn interact with, and affect the positioning and activity of, Innexin gap junctions (Bauer et al., 2002; Bauer et al., 2004; Bauer et al., 2006; Lehmann et al., 2006). These findings suggest that pathological states in insects may occur not just through alteration of gap junctional activity, such as that occurring in *innexin* mutants but also through protein–protein structural and signalling effects. This in turn suggests that the Ichnovirus Vinnexins may in fact alter cell physiology not just through altered gap junctional intercellular communication but also possibly by alteration of host Innexin and other molecule distribution and availability for functioning. However, we currently lack the knowledge on basic cell biology of Vinnexins, as well as host caterpillar Innexins, to test this hypothesis.

To address this lack, we examined transcript patterns for both CsIV *vinnexins* and a prevalent host caterpillar *innexin* homologue, *innexin2*, in CsIV-infected larvae of *Heliothis virescens* (Lepidoptera:Noctuidae). We then examined Vinnexin and Inx2 proteins alone and in tandem to investigate possible effects of Vinnexin presence on Inx2 cellular localization. Our findings suggest not only that Vinnexins utilize similar cellular machinery for cellular localization as Inx2, and co-localize with Inx2 but also that Vinnexins may affect Inx2 distribution in a protein-specific manner. These findings provide groundwork for future analyses of Vinnexin-specific roles in host system manipulation by Ichnoviruses, as well as further exploration of the role of Innexins in coordination of macromolecular scaffolds in insect cells.

Results

Innexin2 and Vinnexin transcript patterns

Transcripts of all four CsIV *vinnexins* are detected in tissues from parasitized *H. virescens* caterpillars (Turnbull et al., 2005). Here, we used QRT-PCR to examine time course and tissue expression patterns. In whole body samples from CsIV-infected *H. virescens*, we observed detectable *vinnexin* transcripts at 3 h post-parasitization (pp), peak transcript titers at 12 h pp, and then a decline throughout the course of parasitoid development (9 days pp)

(Fig. 1A). We quantified transcript titre of the *H. virescens innexin2* orthologue, *hv-inx2*, in *C. sonorensis* parasitized individuals and found that the pattern of *hv-inx2* in parasitized larvae mirrored that of the *vinnexins*, with transcript titre in infected *H. virescens* peaking at 12 h pp. Surprisingly, *vnxG*, the most reliable and strongest coupler in paired *Xenopus* oocytes (Turnbull et al., 2005; Marziano et al., 2011), exhibited the lowest transcript titers among the *vinnexins* in all tested time points; *hv-inx2* likewise had low transcript titers. Peak whole body transcript value (12 h pp) for each gene was inversely correlated to conductance value (Figure S1), suggesting that expression levels of CsIV *vinnexins* may act to compensate weaker conductance levels. The relationship extends to *inx2*: a merged analysis of *hv-inx2* (transcript values) and *S. frugiperda-inx2* (*sf-inx2*; oocyte conductance values) indicates, likewise, there may be an offset of transcript abundance and conductance value.

Tissue-specific transcript titers were then examined for the four *vinnexins*. We generally observed the same ranking of *vinnexin* transcript values (*vnxD* >*vnxQ1* = *vnxQ2* > *vnxG*) as in whole body samples (Fig. 1B). Levels were highest in haemocyte samples. Comparing transcript levels within tissue, there is some evidence of differential regulator effect across genes: *vnxD* transcript titers, for example, are greater than *vnxQ1* in most tissues, but they are equivalent in haemocyte samples.

Innexin2 and Vinnexins localization and trafficking

We focused subsequent analyses on VnxG and VnxQ2 given their distinct transcriptional (Fig. 1), electrical (Turnbull et al., 2005; Marziano et al., 2011; Zhang and Turnbull, 2018) and cellular (Hasegawa et al., 2017; Zhang and Turnbull, 2018) profiles. *Sf*-Inx2, VnxG and VnxQ2 localize to appositional membranes of ectopically expressing High Five cells (Hasegawa et al., 2017), VnxG and VnxQ2 to those of Sf9 cells (Zhang and Turnbull, 2018), VnxQ2 to those of infected *H. virescens* haemocytes (Turnbull et al., 2005), and VnxG to those of transgenic *D. melanogaster* embryos (Hasegawa et al., 2017). Although appositional membrane localization and possibly plaque formation was observed in these previous studies, confocal microscopy was not performed, except in the case of VnxQ2 in *H. virescens*. Here, we tested localization patterns in transfected High Five cells using anti-epitope immunoprobing and confocal microscopy. While our results are similar to previous findings, the resolution afforded by confocal microscopy verified what appear to be gap junctional plaques between expressing cells (Fig. 2). At the same time, all three proteins exhibit cytoplasmic levels, suggesting a reservoir of protein that may be trafficked to the cell membrane.

As the above data implied *Sf*-Inx2, VnxG and VnxQ2 localize to the cell surface, we tested this using surface biotinylation. Here, molecules on the surface of the cell, but not in the cytoplasm, are exposed to biotin, enabling differentiation between cytoplasmic and membrane protein

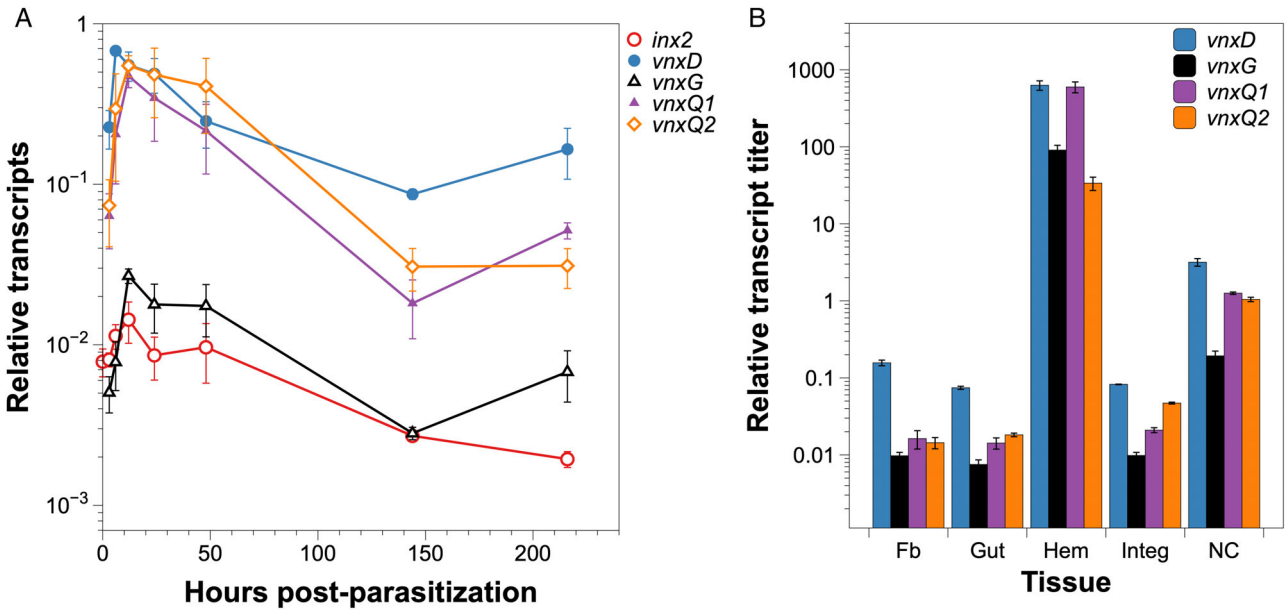

Figure 1. *Vinnexin* and *inx2* transcription in *Heliothis virescens* larvae. (A) QRT-PCR of *vinnexins* and *inx2* from indicated time points prior to and after parasitization by *C. sonorensis*. (B) QRT-PCR of *vinnexins* from different tissues 2 days pp, normalized to 18S rRNA transcript titers. Fb, fat body; Gut, midgut; Hem, hemocytes; Integ, integument; NC, ventral nerve cord.

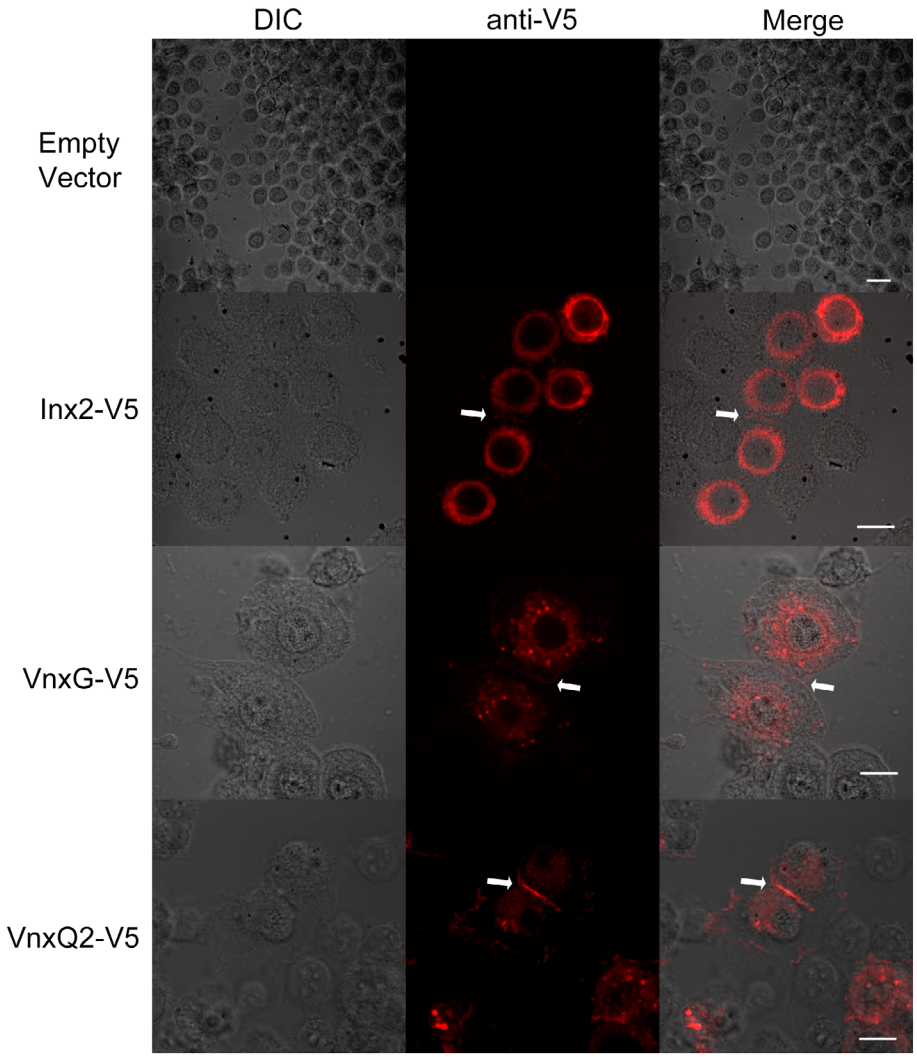

Figure 2. Inx2 and Vinnexins localization in transfected cells. Stable transfections of Inx2-V5, VnxG-V5 and VnxQ2-V5 expressing High Five cells were examined by confocal microscope following anti-V5 immunostaining, 60 h following plating. Arrows indicate probable gap junction plaques between cells. Scale bar = 10 μm.

populations by streptavidin pull-down, followed by western blot. *Sf*-Inx2, VnxG and VnxQ2 are all present in both the cytoplasmic (flow-through) and the surface fractions (Fig. 3). These findings buttress our confocal imaging and previous electrophysiology data (Turnbull et al., 2005; Marziano et al., 2011) indicating that all three proteins are capable of trafficking to the plasma membrane to form functional gap junctions and possibly unapposed hemichannels.

Many Connexins (protein subunits of vertebrate gap junctions) are dependent on actin and microtubule networks for localization (George et al., 1999; Martin et al., 2001; Lauf et al., 2002), while Pannexins (chordate homologues of Innexins) are dependent on actin but not

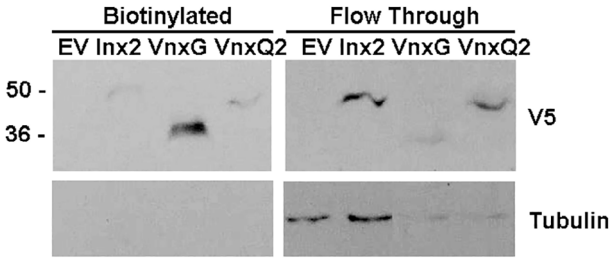

Figure 3. Surface biotinylation demonstrates membrane localization of Innexin2 and Vinnexins. High Five cells stably transfected with the empty pIZT-V5 vector, pIZT/Sf-Inx2-V5 or a *vinnexin* construct were surface biotinylated, treated to streptavidin column and both flow-through (non-biotinylated) and biotinylated fractions analysed by anti-V5 western blot; blots were stripped and re-probed with anti-tubulin to verify the absence of cytoplasmic proteins in biotinylated fractions.

microtubules (Bhalla-Gehi et al., 2010). However, there are no previous reports indicating whether insect Innexins require the actin and tubulin cytoskeleton for proper localization. Therefore, we tested whether *Sf*-Inx2 shares this same dependency, in addition to VnxG and VnxQ2. We inhibited actin and tubulin polymerization with cytochalasin B and nocodazole treatment, respectively, in High Five cells stably transfected with pIZT/inx2-V5-His, pIZT/vnxG-V5-His and pIZT/vnxQ2-V5-His. Following treatment, we visualized the epitope-tagged proteins using anti-V5 immunomicroscopy. Patterns of all three proteins were disrupted severely by both inhibitors (Fig. 4). In particular, all three proteins exhibited a reduction in apparent surface localization in general, and plaque formation specifically. There also appeared fewer cytoplasmic aggregates of protein. Thus, the results indicate that insect Innexins, like Connexins and Pannexins, require both the actin and microtubule networks for proper cellular localization.

Vinnexins co-localize with and may differentially affect Sf-Inx2 localization

As Sf-*inx2*, *vnxG* and *vnxQ2* are transcribed contemporaneously *in vivo* (Fig. 1), and the proteins show similar intracellular distributions (Figs 2–4), we tested them for intracellular co-localization. We generated C-terminal myc-tagged expression constructs for VnxG (vnxG-myc-His) and VnxQ2 (vnxQ2-myc-His) and verified their expression in High Five cells by western blot (data not shown). We then visualized their expression in High Five cells using anti-V5 and anti-myc immunomicroscopy, and observed no impact of epitope on localization of either VnxG (Fig. 5) or VnxQ2 (figure not shown). VnxG-V5 and VnxQ2-myc extensively overlapped, while both VnxG-myc and VnxQ2-myc overlapped with *Sf*-Inx2-V5.

Given the degree of apparent cellular co-localization of VnxG and VnxQ2 with *Sf*-Inx2, as well as shared trafficking mechanisms, we tested whether *Sf*-Inx2 localization was altered in the presence of VnxG and VnxQ2 in real-time with live cell imaging. *Sf*-Inx2 was first expressed transiently in High Five cells as a C-terminal fusion to mCherry (mCherry-Inx2) and compared to unfused mCherry in unfixed (living) cells. Unfused mCherry was distributed evenly throughout expressing cells, while mCherry-Inx2 exhibited both cytoplasmic distribution and occasional punctata both at membranes and cytoplasmically (Fig. 6), similar to *Sf*-Inx2-V5-His protein expressed under the same promoter. We next live imaged mCherry-Inx2 localization when co-expressed with Inx2 or one of the Vinnexins, by co-transfecting cells with the mCherry constructs and pIZT-V5-His constructs encoding *Sf*-Inx2, VnxG or VnxQ2; GFP expression under the OpIE1 promoter of the pIZT-V5-His plasmid permitted visualization of cells successfully transfected with those constructs. The unfused mCherry pattern was unchanged by co-transfection with any plasmid (Fig. 7, and data not shown), and mCherry-

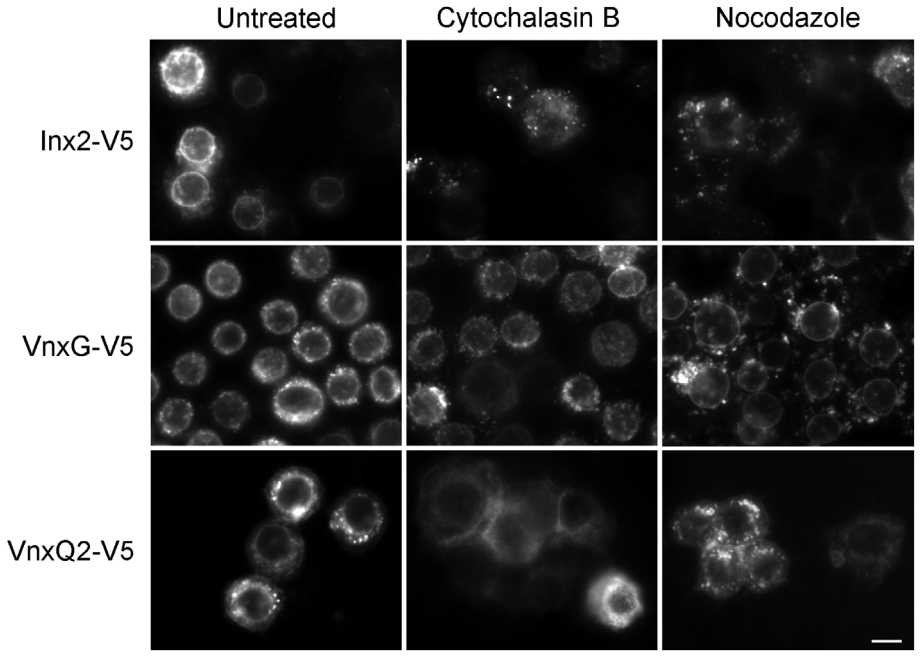

Figure 4. Innexin2 and Vinnexins require actin and microtubule polymerization for proper localization. Inx2-V5 or Vnx-V5 stable expressing High Five cells were subjected to actin or microtubule inhibitors (2.5 μg/ml Cytochalasin B or 10 μM Nocodazole, respectively) 60 h following plating and immunoprobed for V5. Scale bar = 10 μm.

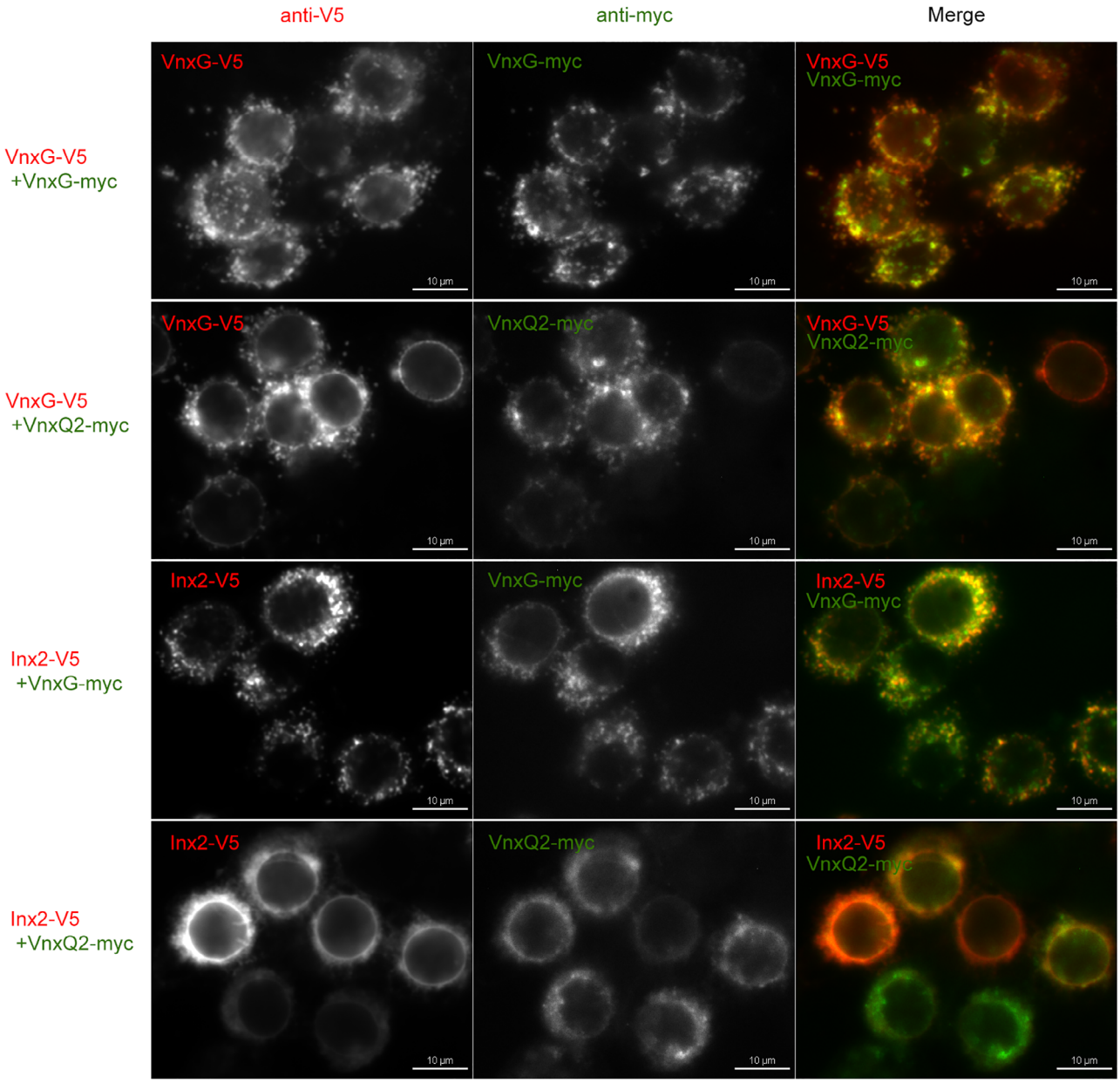

Figure 5. Vinnexins co-localize with *Sf*-Inx2 and each other. High Five cells stably transfected with pIZT/sf-Inx2-V5-His or pIZT/vnxG-V5-His were transiently transfected with pIZT/VnxG-myc or pIZT/VnxQ2-myc. V5 and myc epitopes visualized by immunomicroscopy 36 h after transient transfection. Scale bar represents 10 µm.

Inx2 distribution was unaltered by the empty vector (Fig. 7). Co-expression of either Vinnexin induced greater occurrences of mCherry-Inx2 punctata, with the behaviour more notable in the presence of VnxG than VnxQ2.

We also co-transfected Sf9 cells, which are derived from pupal ovarian tissue of the moth *S. frugiperda* and exhibit more epithelial characteristics, to examine how cell type affects mCherry-Inx2 localization and Vinnexin effect. Again, unfused mCherry was evenly distributed through the cell (Fig. 8), and appeared unaffected by co-transfection (data not shown). The distribution of mCherry-Inx2 was more dispersed throughout Sf9 cells than High Five cells, showing fewer punctata or aggregates and no obvious gap junction plaques. Co-transfection with the empty pIZT or vnxQ2 constructs did not alter Inx2 distribution, while co-transfection with vnxG induced some increased aggregation of mCherry-Inx2 (Fig. 8).

Discussion

Infection by a polydnavirus (PDV) and subsequent expression of PDV genes is essential to the successful

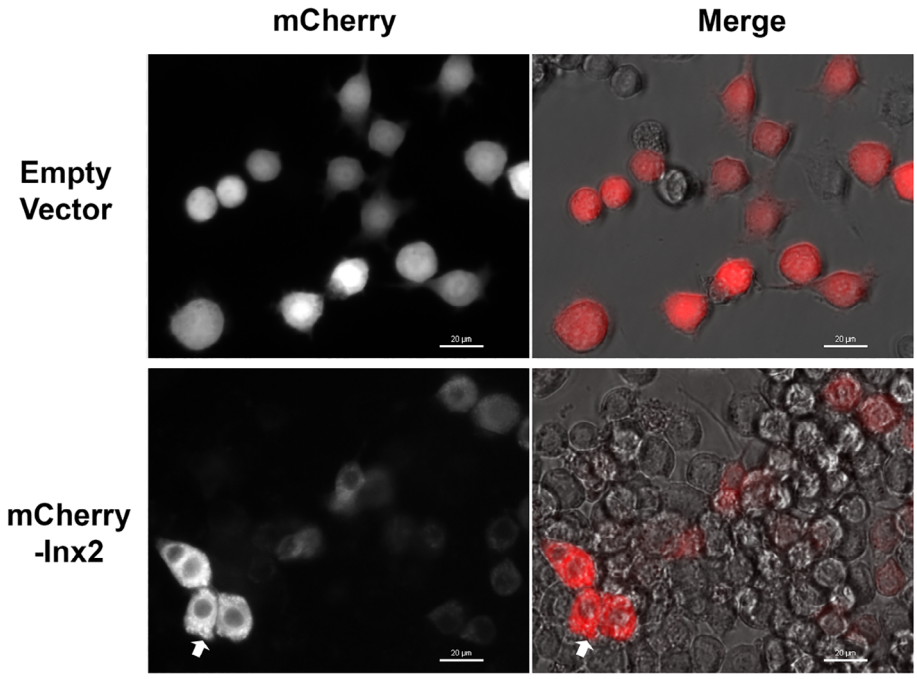

Figure 6. Live imaging of mCherry and mCherry-Inx2 in transfected High Five cells. Cells transfected with the pIZ/mCherry or pIZ/mCherry-Inx2 plasmids were imaged 3 days post-transfection. Arrow indicates punctata in mCherry-Inx2 transfected cell.

parasitization by their associated parasitoid wasp. Consequently, understanding of PDV genome and gene evolution is requisite to explaining wasp host-range evolution. Presumably, despite separate origins, similar life-styles have yielded similar selection regimes on gene family evolution in both Bracovirus and Ichnovirus. Transcript patterns of Bracovirus and Ichnovirus genes across tissues and hosts have led to suggestions that the members play distinct roles in different tissues and hosts, thus contributing differentially to parasitization success. However, while transcriptional analyses have demonstrated variance across permissive and non-permissive hosts (Doremus et al., 2014a; Kim et al., 2015), there is a paucity of functional data particularly in Ichnoviruses testing the theory. Here, we have sought to complement physiological studies of Ichnovirus (specifically CsIV) vinnexins (Marziano et al., 2011; Hasegawa et al., 2017; Zhang and Turnbull, 2018) with cell biological studies to facilitate future studies investigating sub-functionalization within Ichnovirus gene families and its relationship to wasp host-range.

The Ichnovirus cys-motif gene family has long been known to exhibit gene-specific expression patterns, leading to the suggestion that differential expression may result in host- or tissue-specific pathology (Blissard et al., 1987; Blissard et al., 1989). This was tested indirectly across a range of CsIV-susceptibilities, in which expression of the cys-motif protein VHv1.4 correlated with host susceptibility, while the VHv1.4 bound to haemocytes of susceptible, but not non-susceptible, hosts (Cui et al., 2000). Similarly, the seven members of the CsIV viral ankyrin (vankyrin) gene family members exhibit haemocyte- and fat body-preferential transcript counts, a pattern mirrored at the protein level (Kroemer and Webb, 2005). A thorough analysis of *vankyrin* members of Hyposoter didymator IV (HdIV) across hosts and cell lines further identified gene specific expression patterns (Clavijo et al., 2011), supporting the idea that there may be a relationship between gene-specific expression and host susceptibility. This study also suggests both virus- and host-factors may regulate transcript abundance in a gene specific fashion (Clavijo et al., 2011), as was postulated for the CsIV cys-motif gene family (Gill and Webb, 2013).

The *vinnexin* gene family is present in all IVs sequenced to date (Hasegawa and Turnbull, 2014), with members being expressed in permissive hosts (Turnbull et al., 2005; Doremus et al., 2014a; Kim et al., 2015). Expression levels vary across the gene families in all analysed IVs, with some members expressed at higher levels than others. These differentials were consistent both across tissues within host and across hosts in DfIV-infected *Plutella xylostella* and *Phthorimaea operculella* (Kim et al., 2015), while across different species of HdIV-infected larvae, the patterns were inconsistent with some genes expressed at higher levels in some hosts and lower than other *vinnexins* in other hosts (Doremus et al., 2014a).

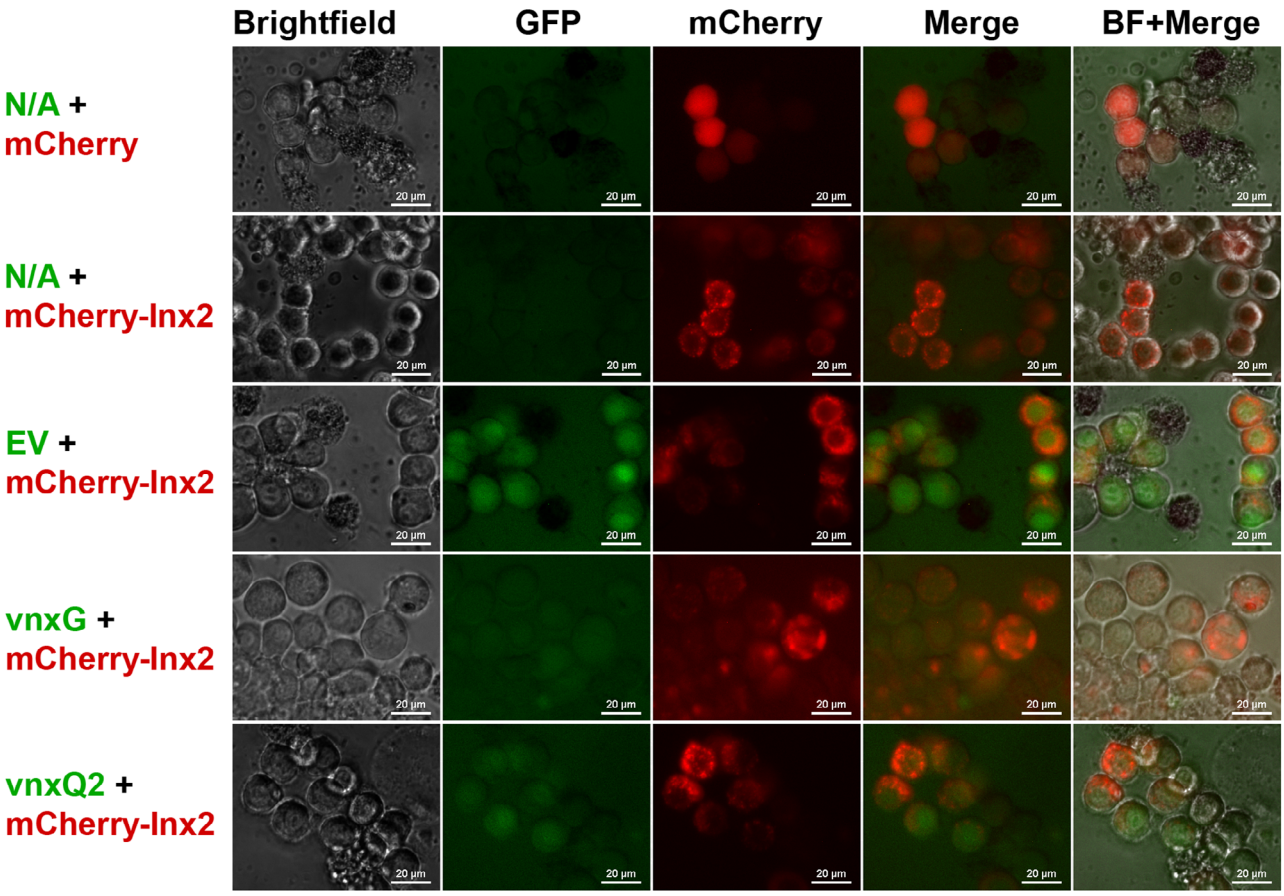

Figure 7. Live imaging of mCherry and mCherry-Inx2 in co-transfected High Five cells. High Five cells transiently co-transfected with constructs to examine localization and potential alteration of subcellular location due to co-expression of vnxG or vnxQ2 on Inx2. GFP channel permits visualization of High Five cells transfected with the various pIZT-V5-His constructs. N/A, no plasmid was co-transfected with pIZ/mCherry or pIZ/mCherry-Inx2; EV, vnxG; vnxQ2, pIZT plasmid cotransfected with pIZ/mCherry-Inx2.

Here, we found fairly consistent transcript titre patterns across tissues within a single host (Fig. 1B), inversely correlating to the ability of the Vinnexin to form functional gap junctions in heterologous systems (Figure S1). These findings imply that there are both *cis*- and *trans*-regulating factors that affect *vinnexin* expression levels, and also support that transcript pattern analysis is insufficient to capture IV gene contribution to host manipulation.

The Innexins are largely supposed to function through formation of hemichannels, which form gap junctions to generate intercellular channels. Gap junctions are present and active in nearly all insect physiological systems, where transfer of small molecules has been observed or is predicted to affect system processes including Malpighian tubule activity (Weng et al., 2008; Piermarini and Calkins, 2014), oocyte patterning and provisioning (Adler and Woodruff, 2000; Anderson and Woodruff, 2001; Bohrmann and Zimmermann, 2008; Kruger and Bohrmann, 2015) and electrical synapse connectivity (Phelan et al., 1996; Phelan et al., 2008; Anava et al., 2009; Anava et al., 2013). Gap junctions also have been observed in the immune system of insects, particularly during transient and continuous contact of haemocytes (Baerwald, 1975; Baerwald, 1979; Caveney and Berdan, 1982; Churchill et al., 1993), while functional data implicate them in haemolytic (Hasegawa et al., 2017) and gut immunity (Li et al., 2014b). At the same time, data indicate that hemichannels can form unapposed channels permitting direct exchange between the environment and cytoplasm (Luo and Turnbull, 2011), possibly playing a role in mediating apoptotic signals in haemocytes (Liu et al., 2013; Li et al., 2014a; Pang et al., 2015). The Vinnexins have previously been demonstrated to form functional gap junctions, including heterotypic (and possibly heteromeric) channels with Inx2 (Marziano et al., 2011), while it remains to be shown that the Vinnexins form functional unapposed hemichannels. Our data here supports that Vinnexins are membrane localized (Figs 1–3), further supporting that Vinnexins function via gap junction and/or hemichannel activity.

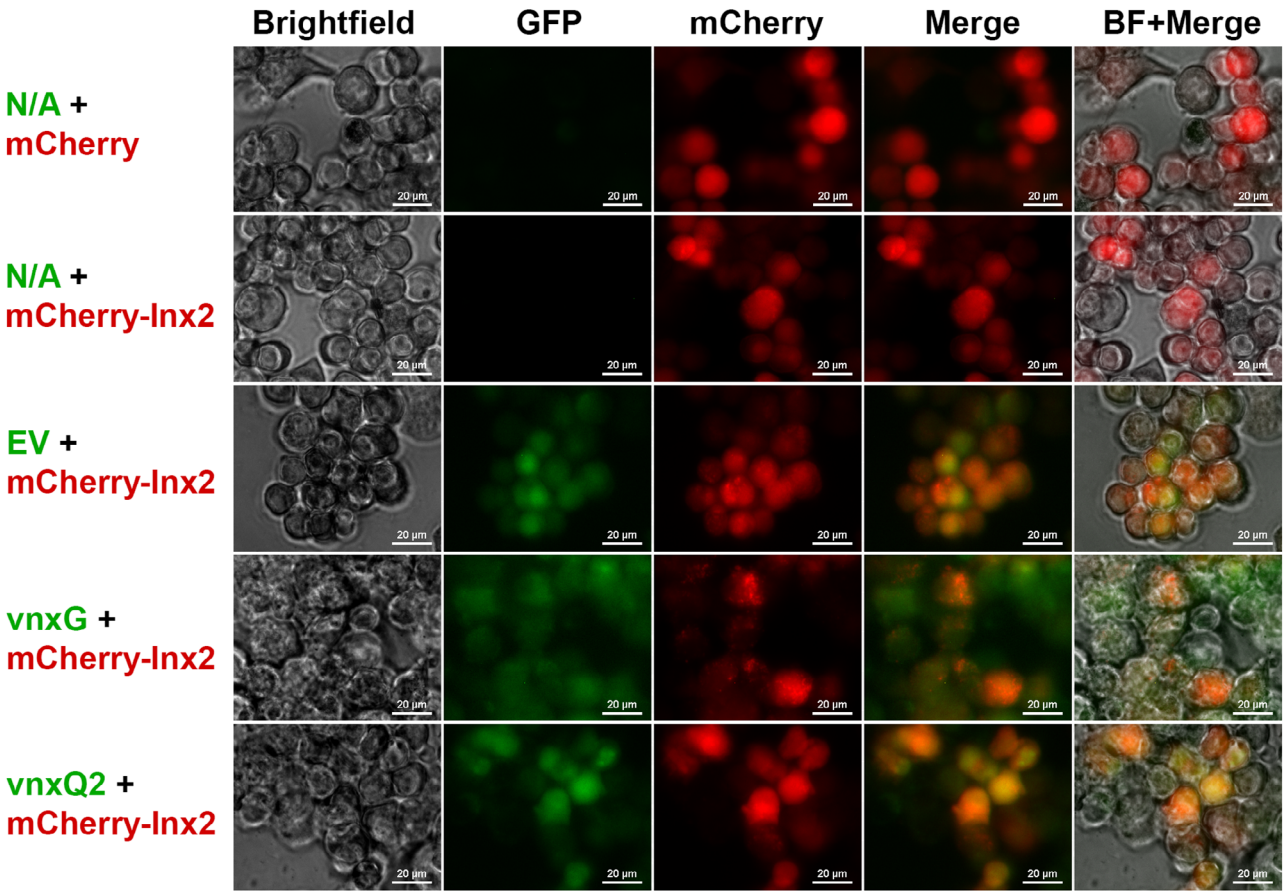

Figure 8. Live imaging of mCherry- and mCherry-Inx2 in co-transfected Sf9 cells. Sf9 cells were transiently co-transfected with empty vector or expression vectors encoding inx2-V5, vnxG-V5 or vnxQ2-V5. GFP channel permits visualization of cell transfected with pIZT-V5-His constructs. N/A, no plasmid was co-transfected with pIZ/mCherry or pIZ/mCherry-Inx2; EV, vnxG; vnxQ2mpIZT plasmid cotransfected with pIZ/mCherry-Inx2.

Intriguingly, though, it may be that the Vinnexins play a role in host pathology not only via altered hemichannel and gap junctional communication but also via alteration of host cellular protein behaviour. While direct protein–protein interaction studies have not been performed, data presented here suggest that VnxG and VnxQ2 differentially interact with host proteins, specifically Inx2. These data are consistent with electrophysiological data (Marziano et al., 2011). Vinnexins appear to utilize broadly the same intracellular trafficking machinery (i.e., actin and microtubule networks) as Inx2 (Fig. 4), and co-localize extensively with Inx2 (Fig. 5). Although not tested quantitatively, imaging suggests VnxG and VnxQ2 may alter Inx2 localization at the membrane (Figs 7–8). This pattern is similar to observations of ectopic Innexin expression in *D. melanogaster*, where interactions of Innexins with other proteins alter localization of the latter typically with negative consequences. For example, *Dm*-Inx2 mutants and Dm-*inx3* RNAi exhibit mis-localization of *Dm*-Inx3 and *Dm*-Inx2, respectively (Lehmann et al., 2006). As well, altered expression of *Dm*-Inx2 or *Dm*-Inx3 lead to altered localization of adherens junction via protein–protein interactions with other junctional components including *D*E-Cadherin and β-catenin (Bauer et al., 2006; Lehmann et al., 2006); conversely, *D*E-Cadherin influences *Dm*-Inx2 localization (Bauer et al., 2006). Consequently, it may be that the Vinnexins alter distribution of other junctional and signalling molecules via protein–protein interactions, thus eliciting host physiological changes.

Here, we have expressed CsIV VnxG and VnxQ2 in conjunction with host Inx2 to examine functional consequences. Our experiments were designed in part due to transcriptional data indicating differences in expression across the *vinnexin* gene family, as well as previous physiological data supporting Vinnexins interact differentially with the host. Our data here indicate that both Vinnexins tested use similar trafficking machinery as *Sf*-Inx2, and overlap extensively in intracellular localization. Further, both proteins appear to potentially alter the cellular localization of *Sf*-Inx2, although to differing degrees. Together,

our data imply that the Vinnexins may disrupt host cell communication via novel gap junction formation, but also via alteration of host-encoded gap junction communication. Further, based on ectopic data from *D. melanogaster* Innexins, the Vinnexins may differentially interact with other host proteins, disrupting host cellular and ultimately organismal physiology.

Experimental procedures

Innexin2 and Vinnexin transcript analysis

Third instar *Heliothis virescens* larvae were subjected to parasitization by *Campoletis sonorensis* as previously described (Turnbull et al., 2005). RNA was isolated from 100 mg tissues or whole body homogenized in Trizol. RNA titers were determined by RiboGreen RNA Quantification Kit (Invitrogen). Isolated RNAs were treated with DNase I (Promega) and absence of gDNA verified by PCR prior to reverse transcription. One microgram of DNA-free RNA was used as template for oligo-dT primed first strand cDNA synthesis using Superscript II (Invitrogen) in 20 μl volume. Quantitative real-time polymerase chain reactions were performed according to published methods (Gill and Webb, 2013): 15 μl reactions with 0.5 μl cDNA template, 200 nM forward and reverse primer and iQ SYBR Green mix (Biorad). Each reaction was set up in triplicate, and performed on a Biorad iCycler thermacycler. Reaction conditions consisted of 40 cycles of 30 sec at 94 °C and 30 sec at 62 °C (*vinnexins* and *inx2*) or 58 °C (*18S*); melt curve analysis was performed after every reaction to ensure single product formation. The primers used were: *hv-inx2*: 5′-AGGCGGTCGCATCAAGATGTTAGT and 5′-GCGTATGCAGGTTTGTGTGGAAGT; *vnxd*: 5′-GGCGATAATTGGTG CGATTGTGGT and 5′-ATCGTCGAGTTGCACTGATCCGAA; *vnxg*: 5′-CGCCGTAGTGTTTCAAAGGCTCAA and 5′-TGAC TCTGGTGTTTCGGATGCTTG; *vnxq1*: 5′-CTGCAACGGAAT ATCAACCCGCTT and 5′-AGTCATTGCCGATGTCAAGCTTGC; *vnxq2*: 5′-TCAATCAGCAGTATGAGTCGTGCG and 5′-TCTCGTCTTGCACAGCACTTTGAG. 18S was used for normalization: 5′-CAGTGATGGGATGAGTGCTTTTATTAGAT and 5′-AGGCCCTCCGTCGATTGGTTTT (Lavine and Strand, 2003). A standard curve was developed from analysis of C_T values of dilution series of cloned full-length cDNAs in pGEM-T Easy, and quantity of cDNA for each transcript determined by the $\Delta\Delta C_T$ method (Perkin-Elmer, 1997). Values for the *hv-inx2* and the *vinnexins* were normalized against 18S values and normalized values were visualized with DataGraph (Visual Data Tools).

Cell line maintenance

High Five cells (Life Technologies) were maintained as adherent cells at 27 °C in TnMFH media (Mediatech) supplemented with 5% FBS. Sf9 cells (Life Technologies) were maintained at 27 °C in serum-free Sf900 III media. Transfections for localization and cytoskeletal inhibitor experiments were performed with Cellfectin II Reagent (Life Technologies) according to manufacturer. Stable transfections were used where noted, and were selected by incubation with zeocin.

Generation of immunofluorescence and live-cell imaging constructs

Synthesis of pIZT-V5-His constructs has been described (Hasegawa et al., 2017). The pIZT/myc-His vector was synthesized from the pIZT/V5-His (Life Technologies) plasmid, using a myc-encoding dsDNA sequence insert following removal of the V5 encoding sequence. Specifically, oligo sequences for myc-encoding region were 5′-GGTTCGAAGAGCAGAAGCTC ATCTCTGAGGAGGACCTCCGTA and 5′-CCGGTACG-GAGGTCCTCCTCAGAGATGAGCTTCTGCTCTTCGAACCGC. The forward and reverse myc oligos were allowed to anneal, yielding dsDNA with terminal SacII and AgeI linker sequences flanking the myc encoding sequence (Glu-Gln-Lys-Leu-Ile-Ser-Glu-Glu-Asp-Leu). pIZT/V5-His was digested with SacII and AgeI, agarose gel isolated, purified, treated with calf intestinal phosphatase (Promega) and ligated to the dsDNA myc oligo. This resulted in a vector with an unchanged MCS relative to the pIZT/V5-His vector, encoding C-terminal myc-6x His product, as verified by sequencing. *VnxG* and *vnxQ2* were subcloned from pIZT/vnxG-V5-His and pIZT/vnxQ2-V5-His, respectively, into homologous sites of pIZT/myc-His to generate pIZT/vnxG-myc-His and pIZT/vnxQ2-myc-His. Correct sequences were verified by DNA sequencing (Clemson University Genomics Institute, CUGI).

A plasmid vector designed to facilitate live imaging of *Sf*-Inx2 in insect cells was generated by inserting mCherry into the pIZ/V5-His plasmid (Invitrogen). PCR amplified (5′-AAGCTTATGGTGAGCAAGGGCGAG and 5′-GGTACCGTA-CAGCTCGTCCATGCCG) and restriction digested mCherry was inserted into the HindIII and Acc65I sites (at the 'N-terminal' end) of the pIZ/V5-His MCS to generate the pIZ/NmCherry vector. The modified plasmid was verified by sequencing (CUGI) and mCherry expression analysis by anti-mCherry western blot. *Sf-Inx2* was PCR amplified (5′-GGATCCATGTTTGACGTATTCG and 5′-TCTAGACTACACACTGTCCTTC), digested and cloned into the plasmid to generate pIZ/NmCherry-inx2. Correct insertion was verified by DNA sequencing (CUGI).

Western blotting and immunomicroscopy

Immunological analyses followed previously published methods (Turnbull et al., 2005; Hasegawa et al., 2017; Zhang and Turnbull, 2018). Briefly, for western blots, cells were resuspended in lysis buffer (25 mM Tris–HCl, pH 7.6; 150 mM NaCl; 1% NP-40; 0.5% TritonX-100; 0.1% SDS + protease inhibitors) and protein concentration determined by Bradford. Samples were diluted in 4X reducing loading buffer, boiled for 10 min at 95 °C, and separated on 10% polyacrylamide gels. Proteins were transferred to PVDF membranes and blocked with 4% dry milk in PBT (PBS + 0.02% Tween-20). Blots were probed with primary antibodies in PBT, washed and probed with secondary antibodies in PBT. Blots were processed for ECL substrate (Pierce) and visualized on film. Primary antibodies used in blotting were mouse anti-V5 (1:2500; Life Technologies) and mouse anti-tubulin (1:100; Developmental Studies Hybridoma Bank); goat anti-mouse HRP-antibody secondary antibody was used at 1:10 000 (Jackson Immunoresearch). For immunomicroscopy, cells were fixed 36–60 h post seeding in PBS plus 3.7% paraformaldehyde, permeabilized with PBST (PBS plus 0.02% TritonX-100) and blocked

with 4% dry milk in PBST. Antibodies were diluted in PBST and included primary mouse anti-V5 1:200 (Life Technologies) and rabbit anti-myc 1:200 (Bethyl Laboratories), and secondary anti-mouse Alexa Fluor 598 (Life Technologies) or anti-rabbit Alexa Fluor 350 (Life Technologies) at 1:1000. F-actin was labelled with Alexa Fluor 488 (Life Technologies), and nuclei with DAPI. Imaging was performed on a Nikon TE2000 fluorescent microscope and processed with NIS Elements BR 3.0 software, or by Zeiss LSM500 inverted confocal microscope.

Testing role of cytoskeleton in trafficking Inx2 and Vinnexins

Cells transiently or stably transfected with the empty pIZT/V5-His plasmid, *sf-inx2*, or a *vinnexin*-construct were subjected to cytoskeleton disruptors to test the role of the cytoskeleton in Innexin trafficking. Cells were incubated for 90 m at 37 °C, 60 h post seeding, with either 2.5 μg/ml Cytochalasin B (Acros Organics) to inhibit F-actin polymerization, or 10 μM Nocodazole (Acros Organics) to inhibit microtubule polymerization.

Biotinylation of surface membrane proteins

High Five cells stably expressing *Sf*-Inx2-V5, VnxG-V5 or VnxQ2-V5 were seeded in 25 mm^2 flasks (Corning) and incubated under normal culture conditions to 100% confluency (60 h). Cells were washed three times with ice cold PBS, pH 7.4, and incubated with 1.5 mg Biotin (Thermo Scientific) in 3 ml PBS for 1 h at 4 °C. Cells were washed with ice cold PBS, centrifuged and resuspended in PBS with protease inhibitors (Thermo Scientific). Cells were sonicated and 1 mg total cell lysates were incubated with Streptavidin agarose beads (Thermo Scientific) for 1 h at 4 °C in PBS to isolate biotinylated proteins. Bead complexes were washed five times with ice cold PBS and resuspended in reducing SDS-PAGE loading buffer. Homogenates were analysed by western blot with V5 antibodies to assess Innexin and Vinnexin cell surface localization; blots were stripped and then probed with anti-tubulin antibody to confirm that biotin labelling was excluded from the interior of cells.

Live cell imaging

Cells were transiently transfected with pIZ/NmCherry or pIZ/NmCherry-inx2, and pIZ/myc-His, pIZT/vnxG-myc-His or pIZ/vnxQ2--myc-His. At 3–4 days post-transfection, cells were imaged using green and red fluorescence filters. Exposure times were kept consistent between treatments within replicate.

Acknowledgements

DKH, PZ and MWT designed the project; DKH and PZ performed expression and immunomicroscopic analyses; DKH performed surface biotinylation experiments; PZ performed live-cell imaging; MWT wrote the manuscript. This work was supported in part by USDA-AFRI award 2006-03787 and Clemson University Project Completion Grant to MWT. DKH was supported by a Clemson University Public Services Activities Next Generation Fellowship. The work was supported in part through Clemson University Creative Inquiry Project #850. The E7 anti-tubulin MAb developed by M. Klymkowsky was obtained from the Developmental Studies Hybridoma Bank, created by the NICHD of the NIH and maintained at The University of Iowa, Department of Biology, Iowa City, IA 52242. The authors thank Dr Yayi Kusumah for assistance with QRT-PCR, Dr Kaijun Luo for assistance in adapting biotinylation assay, Maggie Reilly for cell culture assistance, and Richard Melton, Dr Mike Caterino and Dr Andy Mount for critical comments regarding the work.

DATA AVAILABILITY STATEMENT

The data that support the findings of this study are available from the corresponding author upon reasonable request.

References

Adler, E.L. and Woodruff, R.I. (2000) Varied effects of 1-octanol on gap junctional communication between ovarian epithelial cells and oocytes of *Oncopeltus fasciatus*, Hyalophora cecropia, and *Drosophila melanogaster*. *Archives of Insect Biochemistry and Physiology*, **43**, 22–32.

Anava, S., Rand, D., Zilberstein, Y. and Ayali, A. (2009) Innexin genes and gap junction proteins in the locust frontal ganglion. *Insect Biochemistry and Molecular Biology*, **39**, 224–233.

Anava, S., Saad, Y. and Ayali, A. (2013) The role of gap junction proteins in the development of neural network functional topology. *Insect Molecular Biology*, **22**, 457–472.

Anderson, K.L. and Woodruff, R.I. (2001) A gap junctionally transmitted epithelial cell signal regulates endocytic yolk uptake in *Oncopeltus fasciatus*. *Developmental Biology*, **239**, 68–78.

Baerwald, R.J. (1975) Inverted gap and other cell junctions in cockroach hemocyte capsules: a thin section and freeze-fracture study. *Tissue & Cell*, **7**, 575–585.

Baerwald, R.J. (1979) Fine structure of hemocyte membranes and intercellular junctions formed during hemocyte encapsulation. In: Gupta, A.P. (Ed.) *Insect Hemocytes*. Cambridge: Cambridge University Press, pp. 155–188.

Bauer, R., Lehmann, C., Fuss, B., Eckardt, F. and Hoch, M. (2002) The *Drosophila* gap junction channel gene innexin 2 controls foregut development in response to Wingless signalling. *Journal of Cell Science*, **115**, 1859–1867.

Bauer, R., Martini, J., Lehmann, C. and Hoch, M. (2003) Cellular distribution of innexin 1 and 2 gap junctional channel proteins in epithelia of the *Drosophila* embryo. *Cell Communication & Adhesion*, **10**, 221–225.

Bauer, R., Lehmann, C., Martini, J., Eckardt, F. and Hoch, M. (2004) Gap junction channel protein Innexin 2 is essential for epithelial morphogenesis in the *Drosophila* embryo. *Molecular Biology of the Cell*, **15**, 2992–3004.

Bauer, R., Loer, B., Ostrowski, K., Martini, J., Weimbs, A., Lechner, H. *et al*. (2005) Intercellular communication: the *Drosophila* innexin multiprotein family of gap junction proteins. *Chemistry & Biology*, **12**, 515–526.

Bauer, R., Weimbs, A., Lechner, H. and Hoch, M. (2006) DE-Cadherin, a Core Component of the Adherens Junction Complex Modifies Subcellular Localization of the *Drosophila* Gap

Junction Protein Innexin2. *Cell Communication & Adhesion*, **13**, 103–114.

Beliveau, C., Cohen, A., Stewart, D., Periquet, G., Djoumad, A., Kuhn, L. *et al*. (2015) Genomic and proteomic analyses indicate that banchine and campoplegine polydnaviruses have similar, if not identical, viral ancestors. *Journal of Virology*, **89**, 8909–8921.

Bezier, A., Annaheim, M., Herbiniere, J., Wetterwald, C., Gyapay, G., Bernard-Samain, S. *et al*. (2009) Polydnaviruses of braconid wasps derive from an ancestral nudivirus. *Science*, **323**, 926–930.

Bhalla-Gehi, R., Penuela, S., Churko, J.M., Shao, Q. and Laird, D. W. (2010) Pannexin1 and pannexin3 delivery, cell surface dynamics, and cytoskeletal interactions. *Journal of Biological Chemistry*, **285**, 9147–9160.

Bitra, K., Burke, G.R. and Strand, M.R. (2016) Permissiveness of lepidopteran hosts is linked to differential expression of bracovirus genes. *Virology*, **492**, 259–272.

Blissard, G.W., Smith, O.P. and Summers, M.D. (1987) Two related viral genes are located on a single superhelical DNA segment of the multipartite *Campoletis sonorensis* virus genome. *Virology*, **160**, 120–134.

Blissard, G.W., Theilmann, D.A. and Summers, M.D. (1989) Segment W of *Campoletis sonorensis* virus: expression, gene products, and organization. *Virology*, **169**, 78–89.

Bohrmann, J. and Zimmermann, J. (2008) Gap junctions in the ovary of *Drosophila melanogaster*: localization of innexins 1, 2, 3 and 4 and evidence for intercellular communication via innexin-2 containing channels. *BMC Developmental Biology*, **8**, 111.

Caveney, S. and Berdan, R. (1982) Selectivity in junctional coupling between cells of insect tissues. In: King, R.C. and Akai, H. (Eds.) *Insect Ultrastructure*, Vol. **1**. New York, NY: Plenum Press, pp. 434–465.

Churchill, D., Coodin, S., Shivers, R.R. and Caveney, S. (1993) Rapid *de novo* formation of gap junctions between insect hemocytes *in vitro*: a freeze-fracture, dye-transfer and patch-clamp study. *Journal of Cell Science*, **104**, 763–772.

Clavijo, G., Doremus, T., Ravallec, M., Mannucci, M.A., Jouan, V., Volkoff, A.N. *et al*. (2011) Multigenic families in Ichnovirus: a tissue and host specificity study through expression analysis of vankyrins from Hyposoter didymator Ichnovirus. *PLoS One*, **6**, e27522.

Cui, L., Soldevila, A.I. and Webb, B.A. (2000) Relationships between polydnavirus gene expression and host range of the parasitoid wasp *Campoletis sonorensis*. *Journal of Insect Physiology*, **46**, 1397–1407.

Depriest, A., Phelan, P. and Martha Skerrett, I. (2011) Tryptophan scanning mutagenesis of the first transmembrane domain of the innexin Shaking-B(Lethal). *Biophysical Journal*, **101**, 2408–2416.

Doremus, T., Cousserans, F., Gyapay, G., Jouan, V., Milano, P., Wajnberg, E. *et al*. (2014a) Extensive transcription analysis of the Hyposoter didymator Ichnovirus genome in permissive and non-permissive lepidopteran host species. *PLoS One*, **9**, e104072.

Doremus, T., Darboux, I., Cusson, M., Ravallec, M., Jouan, V., Frayssinet, M. *et al*. (2014b) Specificities of ichnoviruses associated with campoplegine wasps: genome, genes and role in host–parasitoid interaction. *Current Opinion in Insect Science*, **2**, 1–8.

Drezen, J.M., Chevignon, G., Louis, F. and Huguet, E. (2014) Origin and evolution of symbiotic viruses associated with parasitoid wasps. *Current Opinion in Insect Science*, **6**, 35–43.

Espagne, E., Dupuy, C., Huguet, E., Cattolico, L., Provost, B., Martins, N. *et al*. (2004) Genome sequence of a polydnavirus: insights into symbiotic virus evolution. *Science*, **306**, 286–289.

George, C.H., Kendall, J.M. and Evans, W.H. (1999) Intracellular trafficking pathways in the assembly of connexins into gap junctions. *Journal of Biological Chemistry*, **274**, 8678–8685.

Gill, T.A. and Webb, B.A. (2013) Analysis of gene transcription and relative abundance of the cys-motif gene family from *Campoletis sonorensis* ichnovirus (CsIV) and further characterization of the most abundant cys-motif protein, WHv1.6. *Insect Molecular Biology*, **22**, 341–353.

Hasegawa, D.K. and Turnbull, M.W. (2014) Recent findings in evolution and function of insect innexins. *FEBS Letters*, **588**, 1403–1410.

Hasegawa, D.K., Erickson, S.L., Hersh, B.M. and Turnbull, M.W. (2017) Virus Innexins induce alterations in insect cell and tissue function. *Journal of Insect Physiology*, **98**, 173–181.

Holcroft, C.E., Jackson, W.D., Lin, W.H., Bassiri, K., Baines, R.A. and Phelan, P. (2013) Innexins Ogre and Inx2 are required in glial cells for normal postembryonic development of the Drosophila central nervous system. *Journal of Cell Science*, **126**, 3823–3834.

Hong, S.M., Noh, S.K., Kim, K.A., Mitsunobu, H., Mon, H., Lee, J. M. *et al*. (2009) Molecular characterization, localization, and distribution of innexins in the silkworm, *Bombyx mori*. *Molecular Biotechnology*, **43**, 52–58.

Kim, J.I., Kwon, M., Lee, S.H. and Kim, Y. (2015) Parasitism and survival rate of Diadegma fenestrale (Hymenoptera: Ichneumonidae) and DfIV gene expression patterns in two lepidopteran hosts. *Biochemical and Biophysical Research Communications*, **459**, 579–584.

Kroemer, J.A. and Webb, B.A. (2005) Ikappabeta-related vankyrin genes in the *Campoletis sonorensis* ichnovirus: temporal and tissue-specific patterns of expression in parasitized Heliothis virescens lepidopteran hosts. *Journal of Virology*, **79**, 7617–7628.

Kruger, J. and Bohrmann, J. (2015) Bioelectric patterning during oogenesis: stage-specific distribution of membrane potentials, intracellular pH and ion-transport mechanisms in Drosophila ovarian follicles. *BMC Developmental Biology*, **15**(1), 1.

Lapointe, R., Tanaka, K., Barney, W.E., Whitfield, J.B., Banks, J. C., Beliveau, C. *et al*. (2007) Genomic and morphological features of a banchine polydnavirus: a comparison with bracoviruses and ichnoviruses. *Journal of Virology*, **81**, 6491–6501.

Lauf, U., Giepmans, B.N., Lopez, P., Braconnot, S., Chen, S. C. and Falk, M.M. (2002) Dynamic trafficking and delivery of connexons to the plasma membrane and accretion to gap junctions in living cells. *Proceedings of the National Academy of Science of the United States of America*, **99**, 10446–10451.

Lavine, M.D. and Strand, M.R. (2003) Haemocytes from *Pseudoplusia includens* express multiple alpha and beta integrin subunits. *Insect Molecular Biology*, **12**, 441–452.

Lehmann, C., Lechner, H., Loer, B., Knieps, M., Herrmann, S., Famulok, M. *et al*. (2006) Heteromerization of innexin gap junction proteins regulates epithelial tissue organization in *Drosophila*. *Molecular Biology of the Cell*, **17**, 1676–1685.

Li, M., Pang, Z., Xiao, W., Liu, X., Zhang, Y., Yu, D. *et al*. (2014a) A transcriptome analysis suggests apoptosis-related signaling pathways in hemocytes of Spodoptera litura after parasitization by Microplitis bicoloratus. *PLoS One*, **9**, e110967.

Li, M.W., Wang, J., Zhao, Y.O. and Fikrig, E. (2014b) Innexin AGAP001476 is critical for mediating anti-Plasmodium responses in Anopheles mosquitoes. *The Journal of Biological Chemistry*, **289**, 24885–24897.

Liu, T., Li, M., Zhang, Y., Pang, Z., Xiao, W., Yang, Y. *et al*. (2013) A role for Innexin2 and Innexin3 proteins from *Spodoptera litura* in apoptosis. *PLoS One*, **8**, e70456.

Luo, K. and Turnbull, M.W. (2011) Characterization of nonjunctional hemichannels in caterpillar cells. *Journal of Insect Science*, **11**(6), 1–17.

Martin, P.E., Blundell, G., Ahmad, S., Errington, R.J. and Evans, W.H. (2001) Multiple pathways in the trafficking and assembly of connexin 26, 32 and 43 into gap junction intercellular communication channels. *Journal of Cell Science*, **114**, 3845–3855.

Marziano, N.K., Hasegawa, D.K., Phelan, P. and Turnbull, M.W. (2011) Functional interactions between polydnavirus and host cellular innexins. *Journal of Virology*, **85**, 10222–10229.

Pang, Z., Li, M., Yu, D., Yan, Z., Liu, X., Ji, X. *et al*. (2015) Two innexins of *Spodoptera litura* influences hemichannel and gap junction functions in cellular immune responses. *Archives of Insect Biochemistry and Physiology*, **90**, 43–57.

Perkin-Elmer. (1997) *ABI PRISM 7700 Sequence Detection System User Bulletin #2: Relative Quantitation of Gene Expression*. http://tools.thermofisher.com/content/sfs/manuals/cms_040980.

Phelan, P., Nakagawa, M., Wilkin, M.B., Moffat, K.G., O'Kane, C. J., Davies, J.A. *et al*. (1996) Mutations in shaking-B prevent electrical synapse formation in the *Drosophila* giant fiber system. *Journal of Neuroscience*, **16**, 1101–1113.

Phelan, P., Goulding, L.A., Tam, J.L., Allen, M.J., Dawber, R.J., Davies, J.A. *et al*. (2008) Molecular mechanism of rectification at identified electrical synapses in the *Drosophila* giant fiber system. *Current Biology*, **18**, 1955–1960.

Piermarini, P.M. and Calkins, T.L. (2014) Evidence for intercellular communication in mosquito renal tubules: a putative role of gap junctions in coordinating and regulating the rapid diuretic effects of neuropeptides. *General and Comparative Endocrinology*, **203**, 43–48.

Stebbings, L.A., Todman, M.G., Phillips, R., Greer, C.E., Tam, J., Phelan, P. *et al*. (2002) Gap junctions in *Drosophila*: developmental expression of the entire innexin gene family. *Mechanisms of Development*, **113**, 197–205.

Strand, M.R. and Burke, G.R. (2013) Polydnavirus-wasp associations: evolution, genome organization, and function. *Current Opinion in Virology*, **3**, 587–594.

Tanaka, K., Lapointe, R., Barney, W.E., Makkay, A.M., Stoltz, D., Cusson, M. *et al*. (2007) Shared and species-specific features among ichnovirus genomes. *Virology*, **363**, 26–35.

Turnbull, M.W., Volkoff, A.-N., Webb, B.A. and Phelan, P. (2005) Functional gap-junction genes are encoded by insect viruses. *Current Biology*, **15**, R491–R492.

Volkoff, A.N., Jouan, V., Urbach, S., Samain, S., Bergoin, M., Wincker, P. *et al*. (2010) Analysis of virion structural components reveals vestiges of the ancestral ichnovirus genome. *PLoS Pathogens*, **6**, e1000923.

Webb, B.A., Strand, M.R., Dickey, S.E., Beck, M.H., Hilgarth, R.S., Barney, W.E. *et al*. (2006) Polydnavirus genomes reflect their dual roles as mutualists and pathogens. *Virology*, **347**, 160–174.

Weng, X.H., Piermarini, P.M., Yamahiro, A., Yu, M.J., Aneshansley, D.J. and Beyenbach, K.W. (2008) Gap junctions in Malpighian tubules of *Aedes aegypti*. *Journal of Experimental Biology*, **211**, 409–422.

Zhang, P. and Turnbull, M.W. (2018) Virus innexin expression in insect cells disrupts cell membrane potential and pH. *The Journal of General Virology*, **99**, 1444–1452.

Supporting Information

Additional supporting information may be found online in the Supporting Information section at the end of the article.

Figure S1. Transcript titre and gap junctional intercellular communication ability of the Vinnexins and Inx2. Mean whole body transcript titre (±SD) at 12 h, 1 day, and 2 days pp were graphed against mean conductance value (μS ± SEM) in paired *Xenopus laevis* oocytes (Marziano et al., 2011). Lines of best fit are colour coded to sampling period. Equations are: (12 h) $y = 1.13*x^{-0.59}$; (1 day) $y = 1.02*x^{-0.59}$; (2 days) $y = 0.76*x^{-0.65}$.